Ecological Indicators 121 (2021) 107064

Contents lists available at ScienceDirect

Ecological Indicators

journal homepage: www.elsevier.com/locate/ecolind

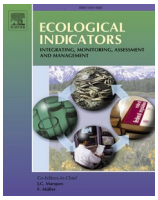

Temperature based indicators to develop adaptive responses for crop production in Florida, USA

Anjali Sharma [a], Aavudai Anandhi [b,*]

[a] School of Environmental Science, Florida Agricultural and Mechanical University, Tallahassee, FL 32307, USA
[b] Biological Systems Engineering, Florida Agricultural and Mechanical University, Tallahassee, FL 32307, USA

ARTICLE INFO

Keywords:
Climate variability
Extreme high temperature change
Crop failure temperatures
Coupled Model Inter-comparison Project Phase5 (CMIP5)
Adaptation strategies
Driver-Pressure-State-Impact-Response (DPSIR)

ABSTRACT

Crop failure temperatures (CFTs) are critical upper threshold temperatures above which plant growth and development stop. Climate variability with CFTs has an essential impact on agriculture, which leads to a decrease in plant yield to nearly zero. This study innovatively combines data analysis and analysis of published literature to develop causal chains/loops using Driver-Pressure-State-Impact-Responses (DPSIR) framework. In data analysis, CFTs trends were estimated from 21 models participating in the Coupled Model Inter-comparison Project Phase 5 (CMIP5) for the historical (1950–2005) and future scenarios (RCP 8.5, 2006–2100) at a spatial resolution of 0.125°x0.125° over Florida region. From the scenario funnel plots, it is evident that the frequency of number days above CFTs was found to be increasing at the rate of 2 days/year, and maximum mean temperature intensity was found in the range of 0.02 to 0.04 °C/year till 21st century. The causal chain and loop help to understand the complex structure and feedback mechanism for CFTs. This also helps in bridging the gap between climate and crop to address the adaptation strategies if the impacts are known. Adaptation strategies from the effects of the crops found to be promising to mitigate the effects of climate on crop and which can be used by the stakeholders and managers for their own use.

1. Introduction

Temperature is one of the critical variables that sustain life on Earth (Anandhi and Blocksome, 2017), with changing and varying temperatures impacting it (Sinnathamby et al., 2018) as well as creating economic losses (Ben-Ari et al., 2018). Increasing temperatures are projected at global scales (Edenhofer, 2015) as well as at regional levels. Average global temperatures reached 1 °C above pre-industrial times in 2015 (Howarth and Monasterolo, 2016). In Florida and Southeastern United States of America (USA), a meta-analysis of the literature showed temperature changes and variability ranged from −3 °C to 6 °C during 1950–2100 (Anandhi and Bentley, 2018; Anandhi et al., 2018). The estimated economic market/nonmarket impact in the United States could be 1.2 percent of gross domestic product per plus 1 °C temperature rise on average (Ba and Galik, 2019). Globally, more frequent and disruptive weather events in 2015 represent 94% of insurance claims (in the last decade), costing >$27 billion (Howarth and Monasterolo, 2016). Abnormally warm temperatures (late autumn) and unusually wet conditions (following spring) in breadbasket in France resulted in meager yields as well as lower exchange prices in 2016, which resulted in ~2.3 billion dollars loss for France (Ben-Ari et al., 2018).

Agricultural production accounts for ~30% of the global energy consumption, ~92% of the human water footprint, and over 20% of global greenhouse gas emissions (Nie et al., 2019). About 795 million people do not get enough food to lead a healthy active life (Keairns et al., 2016), while the global demand for food, energy, and water (FEW) is estimated to increase by over 50% by 2050, compared with 2015 (Zhang et al., 2018). On the other hand, cropland expansion, an adaptation strategy used to meet the increasing food demand by 2050, is expected to reduce from 14% to 10% due to environmental reasons (Nie et al., 2019). Therefore, understanding the causality of changing and varying temperatures on these plant production systems become important.

Although, in the agricultural production systems, plant growth and development is dependent on low (base temperature), mean (optimum), and high temperatures, this study focuses on changes and variability in crop failure temperatures (CFTs), which are the upper threshold temperatures that are very hazardous to the plant. CFT can be defined as the maximum temperature above which crop growth stops, which leads to crop failure (Anandhi and Blocksome, 2017). A closely related term to CFT is plant heat stress, which occurs if plants are exposed to high

* Corresponding author.
E-mail address: anandhi@famu.edu (A. Anandhi).

https://doi.org/10.1016/j.ecolind.2020.107064
Received 6 February 2020; Received in revised form 10 September 2020; Accepted 8 October 2020

temperatures for a sufficient period, causing irreversible impact (Wahid et al., 2007). These threshold temperatures and its influence can vary with the crop (Hatfield et al., 2008) and (Hatfield et al., 2011). Depending on the crop (e.g., cotton, sorghum, maize, peanuts, and beans), it impacts the growth, size, weight, number, and filling duration of boll/seed/grain/nut/kernel/bean; harvest index; indehiscence of anthers; pollen viability and production (Adhikari et al., 2016; Anapalli et al., 2016; Chen et al., 2019; Hall, 1992; Hatfield et al., 2008; Reddy et al., 2005); (Hatfield et al., 2008; Prasad et al., 2006; Srivastava et al., 2010) (Hatfield et al., 2011, 2008; Rotundo et al., 2019) (Ruane et al., 2014; Vara Prasad et al., 2003); (Hatfield et al., 2011, 2008; Pan, 1996; Thomas, 2001); (Gross and Kigel, 1994; Hatfield et al., 2008; Prasad et al., 2002); (Adams, 2001; Hatfield et al., 2008; Peet et al., 1998). Therefore, understanding the trends in the CFTs, its impact on multiple crops are essential, particularly in developing adaptation strategies for utilizing the benefits of change while reducing the harmful effects for sustainable development of plant production systems.

Several adaptation strategies are designed to minimize the impact of CFTs. In this study, three levels of adaptation, i.e., incremental adaptation, system adaptation, and transformational adaptation (Anandhi et al., 2016b) are studied. Incremental adaption -strategies observed in literature are the planting and sowing dates, changing the planting area, water-saving technology, deficit irrigation or changing the frequency of irrigation pattern and management of fertilizers are used for different heat-stressed crops (Byjesh et al., 2010; Kothari et al., 2017; Ventrella et al., 2012; Yang et al., 2014). System adaptation strategies such as changing plant cultivators, developing new cultivars for heat tolerance, lower stomatal sensitivity to elevated CO_2 and water availability, having complete biophysical models of crops interactions with environmental variations, shifting to short or long season varieties (Nhamo et al., 2019; Prasad et al., 2002; Schlenker and Roberts, 2009; Singh et al., 2011). Likewise, transformation adaptation includes the land-use change of the crop or adaptability of other major crops in the region is studied (Chatzidaki and Ventura, 2010; Rockström et al., 2010).

The DPSIR framework will be used to develop causal chains/loops in this study. DPSIR stands for Driver-Pressure-State-Impact-Responses was developed in the late 1990s by the Organization of Economic Co-operation and Development (Linster, 2003). Several methods have been used in previous studies for the adaptation strategies (Jarvis et al., 2011; Neset et al., 2019; O'connell et al., 2015; Smit et al., 1999). This study will innovatively utilize the Driver-Pressure-State-Impact-Responses (DPSIR) framework and CFT indicators to develop the causal chain loop between the changes in temperature to responses (strategies), understanding and representing the cause and effect relationships. Earlier studies from this research group have used CFT (1) as an ecosystem indicator to communicate technical data; (2) to interpret the relationship between the climate and plant growth; (3) to develop the adaptation strategies (Anandhi and Blocksome, 2017); (4) to document the exposure (degree of stress) of plants (Anandhi, 2016); (5) to access vulnerability of water resources in agro-ecosystems (Anandhi and Kannan, 2018). Although trends of high frequency and the extreme event of heat stress are already discussed in several studies (Anandhi and Blocksome, 2017; Wang et al., 2016), they are a lacuna of studies in Florida.

This study addresses the question: Will climate impact on the crop bridges the gap with adaptation strategies with the help of crop failure temperature as an indicator? To understand this question, the objectives of this study are twofold. The first is to document the variation and changes in frequency and intensity of CFT for several crops grown in Florida. Second to develop the causal chains/loops that link the climate with the plant, which brings out the cause and effect relationships between how the different drivers and pressures interact and lead to impacts and responses using the Driver-Pressure-State-Impact-Responses (DPSIR) framework. This can lead to the sustainable development of agro-ecosystems by reducing vulnerability while increasing its adaptation capacities to cope with stress. This provides information for the development of adaptation strategies for agriculture and crops in a variable and changing environment.

2. Study area, datasets used and methodology

The methodology section involved a five-step process: Study scope, data set used, estimation of mean temperature followed by determination of change, development of spatial, temporal, and funnel scenarios using MATLAB programming and finally development of causal chain and loops with the help of DPSIR framework. Moreover, scenarios are studied for the CFTs in terms of intensity and frequency. In this study, the frequency was represented by the number of days in a time period with any temperature larger than or equal to the given crop failure temperature. The intensity was explained by the average maximum temperatures during the day with a maximum temperature greater than or equal to the CFT.

2.1. Study area

Florida State in the southeastern USA is chosen as a study area (Fig. 1). Florida is recognized as 'sunshine state' because the summer is very long and moist (Henry, 1994). Studying CFTs in Florida is useful because it has many endemic plants, vertebrates, and insects that are only found in Florida and the tropics. Florida is also the major consumer of water, where the main source of the irrigation is from the surface and groundwater, which is due to the rainfall to grow crops (Marella, 1999). Further, the agricultural production in the region is an essential economic driver for the state's economy and ranks seventh in the USA of farming exports with over $4 billion in agriculture commodities shipped in 2015. Florida plays a vital role in vegetable and fruit production. For example, the state ranks first for fresh market snap bean, cucumber, grapefruit, oranges, sugarcane, tomatoes, and watermelon production; second in production of bell peppers, sweet corn, squash, and strawberries; third in production cabbage and honey; and fourth in peanuts (FDACS, 2017). Overall, the state accounts for roughly 54% of total USA citrus production (Usda-Nass, 2017) and contribute 63% of the winter vegetables for the United States with revenues of $1.48 billion in 1995–1996 (Cheng et al., 2015). This region is highly vulnerable to increasing high temperatures (Anandhi et al., 2018; Anandhi and Bentley, 2018), which affects the yield and production of crops.

2.2. Datasets used

Daily simulations of maximum surface temperature from 21 Global Climate Model (GCMs, Table S1) from Coupled Model Intercomparison Project Phase 5 (CMIP5) were used in this study (Maurer et al., 2002). For further detail, check the link: http://www.engr.scu.edu/~emaurer/data.shtml. Results from historical (1950–2005) and future (2006–2100) experiments were investigated. The represented concentration pathway (RCP 8.5) scenario was considered in the study because it followed the historical/present forcing of the global CO2 emissions (Bhardwaj et al., 2018; Peters et al., 2013). This dataset was at $0.125^\circ \times 0.125^\circ$ grid resolution for the complete USA, from which the Florida domain data were extracted with 856 grids. Additionally, the various threshold CFTs for multiple crops grown in Florida were used (Table 1).

2.3. Methodology

2.3.1. Analyzed maximum temperature from CMIP5 model simulations

The annual and monthly plots of daily maximum surface temperatures from all 21GCMs model simulations (listed in Table S1) were developed from daily values. Annual scenarios were illustrated, consisting of one temperature value for each year and corresponding for each simulation model for historical and RCP 8.5 time period. Similarly, monthly climatology from maximum surface temperature is illustrated,

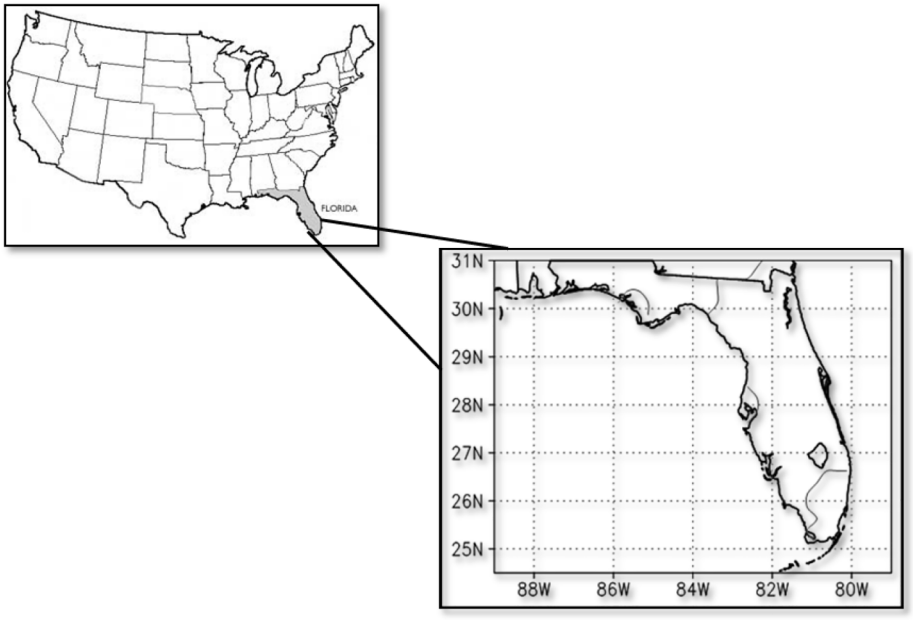

Fig. 1. The study region.

Table 1
Crop failure temperature for vegetative and reproductive development of selected crops adapted from Hatfield et al. (2008) and Anandhi and Blocksome (2017).

Plant name	Plant Failure Temperature
Tomato	30 °C
Bean	32 °C
Maize	35 °C
Peanut, Soybean, Sorghum, Cotton	39 °C
Grass	40 °C

showing only the monthly boxplots developed by estimating the mean daily maximum temperature for each month during the same 1950–2100 time period. Each boxplot constitutes from values of 21 models for a month computed by area averaging over 856 grid points of Florida.

2.3.2. Analyzing the variability of CFTs

CFT were estimated for each GCM. For each grid and year, the number of days in a month with Tmax ≥ CFT was counted using MATLAB programming, which represents frequency. Similarly, for each year and grids, when the temperature exceeds, the selected CFT were averaged to get the intensity of CFTs. For each of the crop failure temperatures (Table 1), the mean values for each of the simulation models were estimated. This was demonstrated through a boxplot of the values, used to observe the interquartile range (lowest-25th and highest-75th percentile).

2.3.3. Assessed annual trends in CFTs:

For analyzing annual trends, linear regression lines were fitted for the six CFTs (30 °C, 32 °C, 35 °C, 39 °C and 40 °C) for a total number of 856 grids, 21 model simulations and three different periods each for six time periods. These are referred as six time-periods in the rest of the manuscript. For more details of these trend estimations, please refer to (Anandhi and Blocksome, 2017). Linear regression lines were fitted to each of these time series to estimate trends. The slope of the fitted line or the linear trend value was given as:

$$slope = \frac{\sum (t-\bar{t})T_t}{\sum (t-\bar{t})^2} \quad (1)$$

where T_2 was the predictions (e.g., T_{max} and CFTs), and n was the number of data points, i.e., year to year. The denominators of Eq. (1) are estimated using Eq. (2).

$$\sum (t-\bar{t})^2 = \frac{n(n^2-1)}{12}. \quad (2)$$

The t^{*} followed the t-distribution and was compared with critical t values at a significance level ($\alpha = 0.05$) with (n-2) degrees of freedom. The ratio between the estimated trend and its standard error (S_{slope}) was calculated to test if the trends in T_t were significantly different from zero and represented by:

$$t^{*} = \frac{slope}{S_{slope}} \quad (3)$$

S_{slope} was calculated using Eqs. (4) and (5) below, representing the variance of the residuals (Pagan et al., 2020), with equivalent sample size n_c to account for lag one serial autocorrelation (r_1) in the time series showing a correlation between values that are one time period apart.

$$S_{slope} = \frac{1}{n_c - 2}\sum (T_t - \hat{T}_t)^2 \quad (4)$$

$$n_c = n\frac{1-r_1}{1+r_1} \quad (5)$$

2.3.4. Developed the spatiotemporal plots for CMIP5 model simulations

The spatiotemporal analysis was done to compare the variations in the slope of the number of days (Frequency) and the mean of temperature (Intensity) above CFTs. The spatial plot is a filled contour plot containing the isolines of intensity or frequencies of various CFTs. Isolines represent lines of equal intensity and frequency for each CFT. The number of days for each CFT was estimated for three time periods each for historical, i.e., 1950–1975, 1976–2005 and 1950–2005 and RCP 8.5 i.e., 2006–2050, 2050–2100 and 2006–2100 were plotted. Their significant median trends for the spatial distribution of frequency and intensity were plotted for the six CFTs, and three-time periods each for historical and RCP 8.5 are plotted.

2.3.5. Synthesized the funnel plots among the 21 CMIP5 model simulations

The trends in the frequency and intensity of the three-time periods

each for the four time periods (1950 to 1975, 1976 to 2005, 2006 to 2050, 2051–2100) were synthesized using funnel plots and a range of trend values. These form the boundary of the funnel plots. Detailed explanation in developing the funnel plot can be obtained from Bentley and Anandhi (2020), Anandhi et al. (2018) and Anandhi et al. (2016a).

2.3.6. *Development of causal chain/ loop using DPSIR framework*

Causal loop diagrams (CLDs) were used to map the variables (components), relationships, and feedback loop (Binder et al., 2004; Zare et al., 2019). According to Sterman (2010), it is generally used to map and communicate problems the problem structure and eliciting individual and team mental models. The main advantage of using CLDs is that they are flexible framework where creators identify and describe, in increasing levels of complexity, the cause-effect relationships of different sub-components of a more extensive system and to understand its feedback mechanisms (Haraldsson, 2004; Ness et al., 2010). Arrows are used to link cause-effect relationships, connecting the two components to develop the causal chain and loops. The diagrams use different symbols to denote different relationships. A definite plus [+] logo between two variables indicates a parallel behavior of the two, meaning an increase in the causative variable also causes the effect variable to increase; furthermore, a decrease in the causative variable denotes a reduction in the affected variable. Conversely, a negative minus [−] logo indicates an inverse relationship between the two variables, meaning as the causative variable increases, the affected variable decreases, or vice-versa.

The DPSIR framework helps to organize and structure indicators in the context of a so-called causal chain that links indicators of the environmental driving forces, to pressure indicators, to environmental state indicators, to impact indicators, and finally to the indicator of responses (Niemeijer and de Groot, 2008; Pagan et al., 2020). In this study, driver refers to important activities that have a direct impact on the environment; pressures result from the driving force which impacts the state; state refers to the condition of the environment that is not static; Impacts are the changes in the states, and finally, the responses indicate to formal efforts to address changes in state, impact, and pressures. The responses in this study are the adaptation strategies defined as "the general plan or some action for addressing the impact of climate change, including climate variability and extremes, which includes varied policies and measures with a specific objective to reduce vulnerability"(Biesbroek et al., 2010). This framework is based on causality (cause-effect) that has important benefits to make responses (adaptation strategies) based on literature review. Incorporation of DPSIR framework (Fig. 2b) with the CLDs will show the complex cause and effect linear and non-liner relationship, that will able to deal with dynamics (trends), different spatial scales and thematic boundaries (Vannevel, 2018).

3. Results

3.1. *Changes in maximum temperature from CMIP5 models*

From Fig. S1a, the annual surface maximum temperature from 21

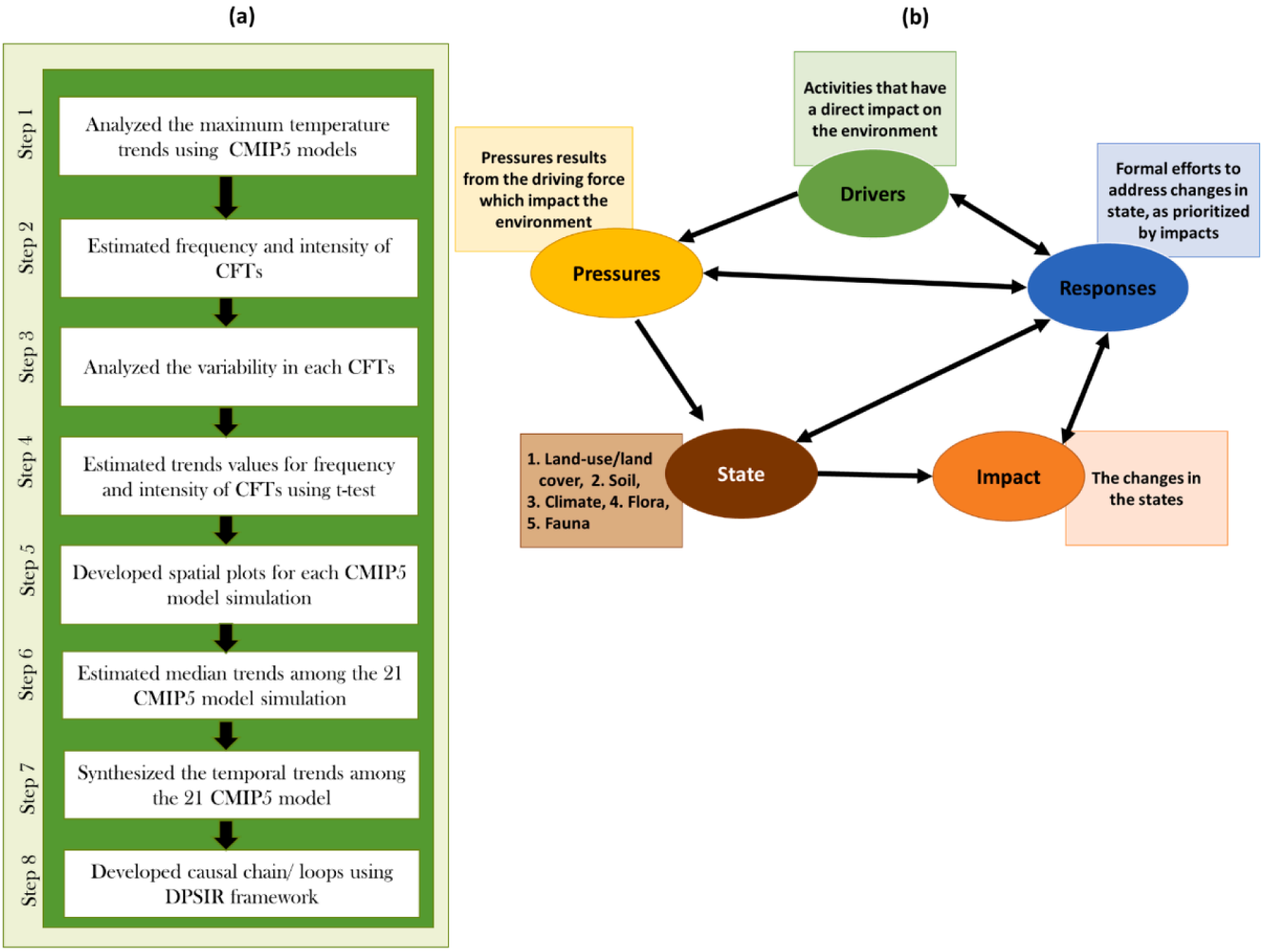

Fig. 2. **(a)** Flowchart is showing the methodology. The acronyms in the figure: CFTs is crop failure temperature, CMIP5 is Coupled Model Inter-comparison Project Phase 5 **(b)** The DPSIR Framework used in the study (Adapted from Anandhi et al., 2018).

CMIP5 model simulations during the 1950–2100 time period, it can be observed that the maximum surface temperature increased in the range 3.5 °C to 5 °C. The simulated temperatures were in the range 27 °C to 28 °C during 1950, later increased to 30 °C and 32 °C during 2100. The variability among the models range from 0.8 to 2 °C during 1950–2100, was observed from the width of the shaded portion in the figure.

The boxplots (Fig. S1b) shows the monthly temperature variability for historical and RCP 8.5. The highest average temperatures of 33 °C in July and the lowest average temperature of 21 °C in January were analyzed for the historical period (1959–2005). While the highest average temperature of 35.5 °C in July and the lowest average temperature of 22.2 °C in January was observed in the RCP 8.5 time period (2006–2100). The temperature for the RCP 8.5 scenario during 2006 to 2100 time period (upper boxplots in Fig. S1b) shows a change in temperature of 2.5 °C in July month and 1.2 °C in January month.

3.2. Analyses of intensity and duration of CFTs

The interquartile range (IQR) [lowest 25th percentile – highest 75th percentile] for the Tmax ≥ 30 °C is from [145–170] days, respectively, and for Tmax ≥ 32 °C is from [70–110] days. The IQR is decreasing as we increase the CFT threshold, which reduces to the range from [1–10] days for Tmax ≥ 35 °C and zeros for Tmax ≥ 39 °C and Tmax ≥ 40 °C. For RCP 8.5 (2006–2100), the mean annual frequency shows the increasing trend for all CFTs. The IQR increases in the range of [160–247] days; [98–220] days; [23–183] days; [2–165] days; [0–63] days; [0–31] days for Tmax ≥ 30 °C; Tmax ≥ 32 °C; Tmax ≥ 34 °C; Tmax ≥ 35 °C, Tmax ≥ 39 °C and Tmax ≥ 40 °C respectively. The Tmax ≥ 39 °C and Tmax ≥ 40 °C the frequency only happen after years 2051 and 2066, indicating more CFTs can be observed in future. This plays a significant contribution in the preparation of adaptation strategies till 2100. Fig. 3 shows higher the CFTs lowers the frequency of days were seen in each CFTs.

In general, the intensity boxplot for different CFTs (Fig. 4) during historical (1950–2005), show an increase. The IQR for intensity was 31.6–32.4 for Tmax ≥ 30 °C, 32.8–33.3 for Tmax ≥ 32 °C, 34.3–34.6 °C for Tmax ≥ 34 °C and 35.3–35.4 °C for Tmax ≥ 35 °C. For Tmax ≥ 39 °C, the intensity was 39.2–39.4 °C towards the later part of the 20th century and zero intensity for Tmax > 40 °C . The change in the mean intensity of temperatures was observed due to the difference in the temperature. In RCP 8.5 (2006–2100), the increased intensities were 32–36 for Tmax ≥ 30 °C, 33–37 for Tmax ≥ 32 °C, 34.5–37 for Tmax ≥ 34 °C, 35.5–37.7 °C for Tmax ≥ 35 °C, for Tmax ≥ 39 °C the intensity was 39.3–40 °C after years 2066 and for Tmax ≥ 40 °C was 40.6–40.7 °C after the year 2080.

3.3. Spatiotemporal changes in the median frequency and intensity for CFTs in 21 CMIP5 model simulations

Here in this section, the median of all the models was shown for the trends, as shown in Figs. 5 and 6 for frequency and intensity, respectively. In Fig. 5, the median of all the models trend value for frequency in historical and RCP 8.5 time period. From 1950 to 1975, almost no significant trend for all the CFTs threshold in 1950–1975, which means there was no change in the increase or decrease in the number of days can be observed. From 1976 to 2005, there was an increase in trends that ranged from 0.2 to 1 days/year for the CFTs 30, 32, 34, and 35 °C, whereas, in CFT 39 and 40, no significant trend was seen because there was no number of days estimated above these thresholds. Moreover, from 1950 to 2005 trend for the entire historical period (1950–2005) shows lower values in the range of 0.2–0.4 days/year compared to the 1976–2005 time period, which was consistent due to no significant increase during the 1950–1975 period. Similarly, significant trends were shown for the RCP 8.5 time periods. From 2006 to 2050, there was an increasing trend in the range of 0.2–1 days/year for 30,32, 34, and 35 °C, but no significant trend was seen for 39 and 40 °C. From 2051 to 2100, the increase in trends was shown for all the CFTs in the range of 0.2–1 days/year. Moreover, from 2006 to 2100 the complete RCP 8.5 time period (2006–2100) shows the increase in the trend range from 0.2 to 1 days/year for all the CFTs.

However, the spatiotemporal variability of the frequency and intensity for each GCM was shown in the Supplementary material (Figs. S2–S45) for the historical and RCP 8.5 time periods.

Fig. 6 shows the median of all the models trend value for intensity in historical and RCP 8.5 time period. From 1950 to 1975, the trend values for the 30, 32, and 34 °C were in the range of −0.002 to 0.002 °C/year since there was no increase in temperature change recorded during 1950–1975, which clear exact the reason for having no trends for the 35, 39 and 40 °C. From 1976 to 2005, the temperature threshold of 30, 32, and 34 °C shows the only significant increase in temperature trends ranged from 0.002 to 0.01 °C/year. From 1950 to 2005, shows the complete historical trend for the intensity ranged from 0.002 to

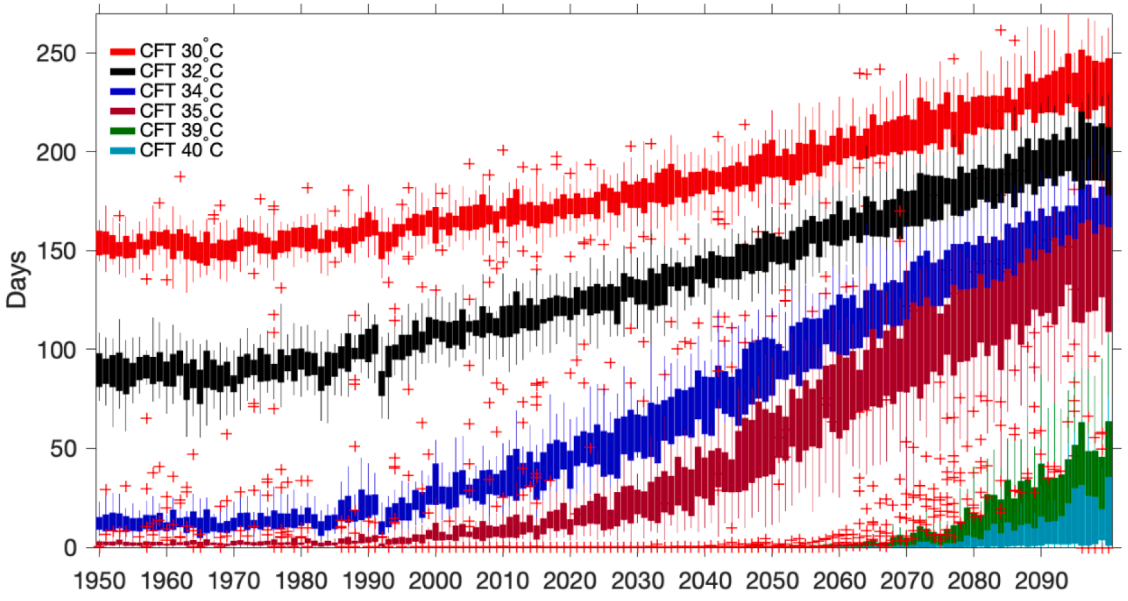

Fig. 3. Variability in the days for each crop failure temperatures (30 °C, 32 °C, 35 °C, 39 °C and 40 °C).

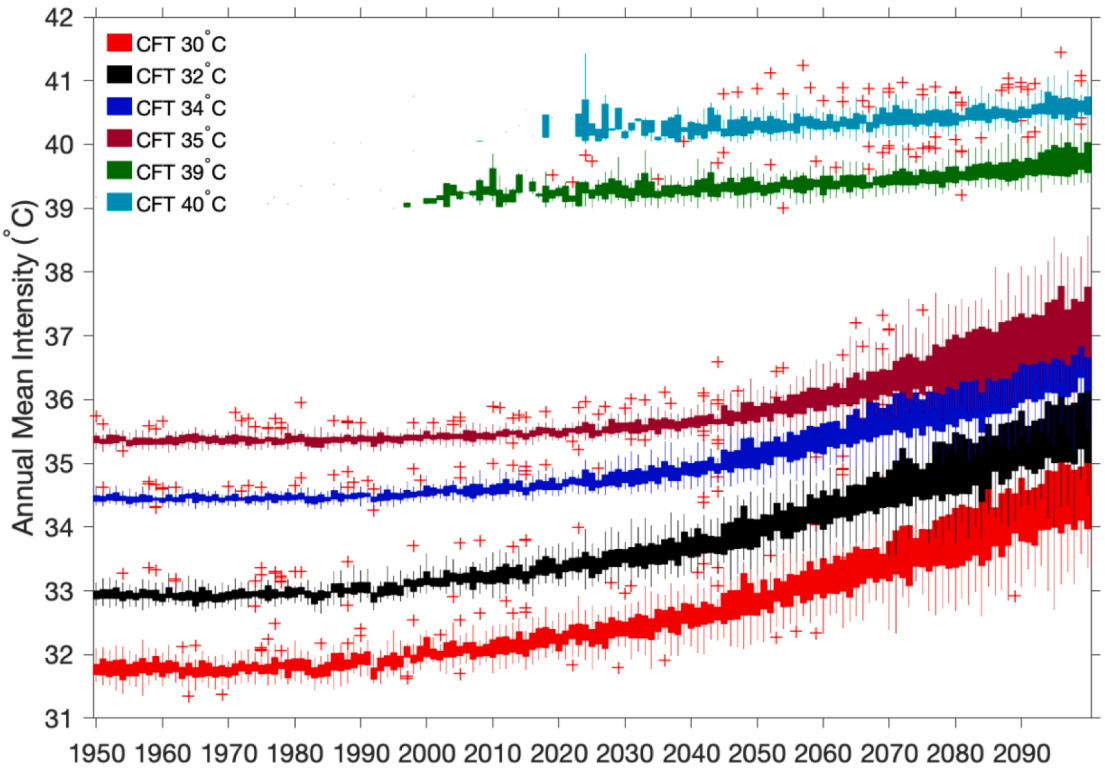

Fig. 4. Variability in the annual mean intensity for each crop failure temperatures (30 °C, 32 °C, 35 °C, 39 °C and 40 °C).

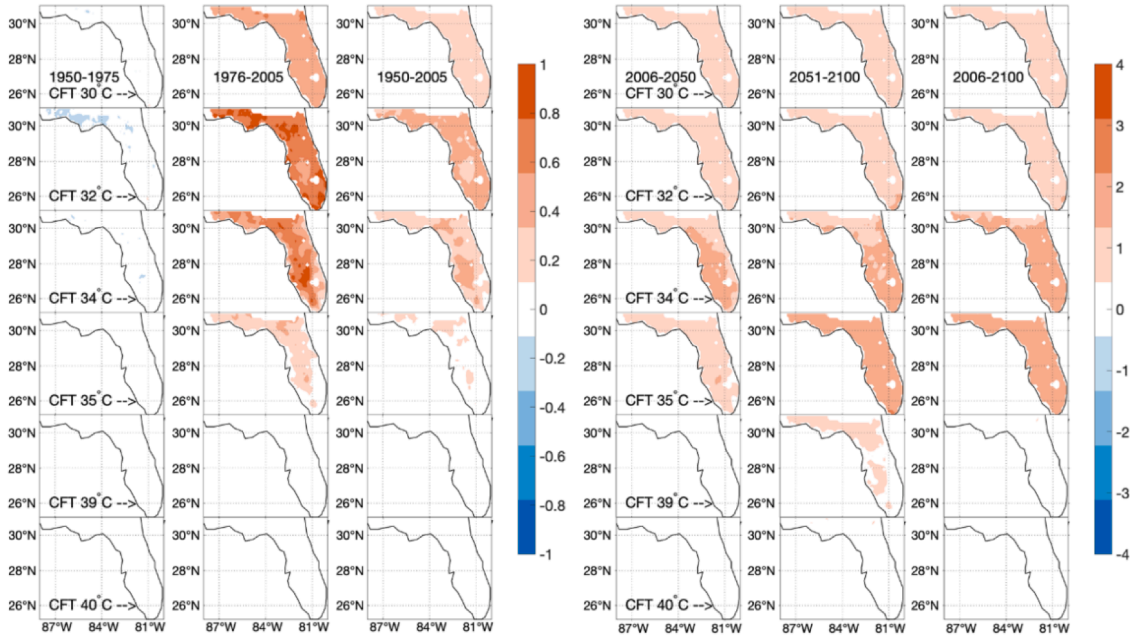

Fig. 5. Median frequency plots for historical simulation first three columns (1950–1975; 1976–2005 and 1950–2005) and RCP 8.5 in the last three columns (2006–2050; 2051–2100 and 2006–2100). Statistical significance was tested with a *t*-test at a confidence interval of 90%.

0.004 °C/year for 30, 32, and 34 °C. Similarly, for the RCP 8.5 time period were shown. From 2006 to 2050, there was an increasing trend in the range of 0.02 °C for 30, 32, and 34 °C but no significant trend was seen for 35, 39, and 40 °C. From 2051 to 2100, the increase in trends was shown for all the CFTs in the range of 0.2–1 days/year. Moreover, from 2006 to 2100 the complete RCP 8.5 time period (2006–2100) shows the no trend range for all the CFTs.

3.4. Development of scenario funnel plot for the trends

Fig. 7 shows the funnels plot i.e made by the changes in trend lines drawn between the years of intervals 1950–1975 and 1975–2005 for the each CFTs. For 30 °C, it shows the trends over all the models and for all the grid points in the range from −0.75 to 0.76 days/year for the 1950–1975 time period and which increases its minimum and maximum values from −0.2 to 1.24 day/year respectively for 1976–2005 time

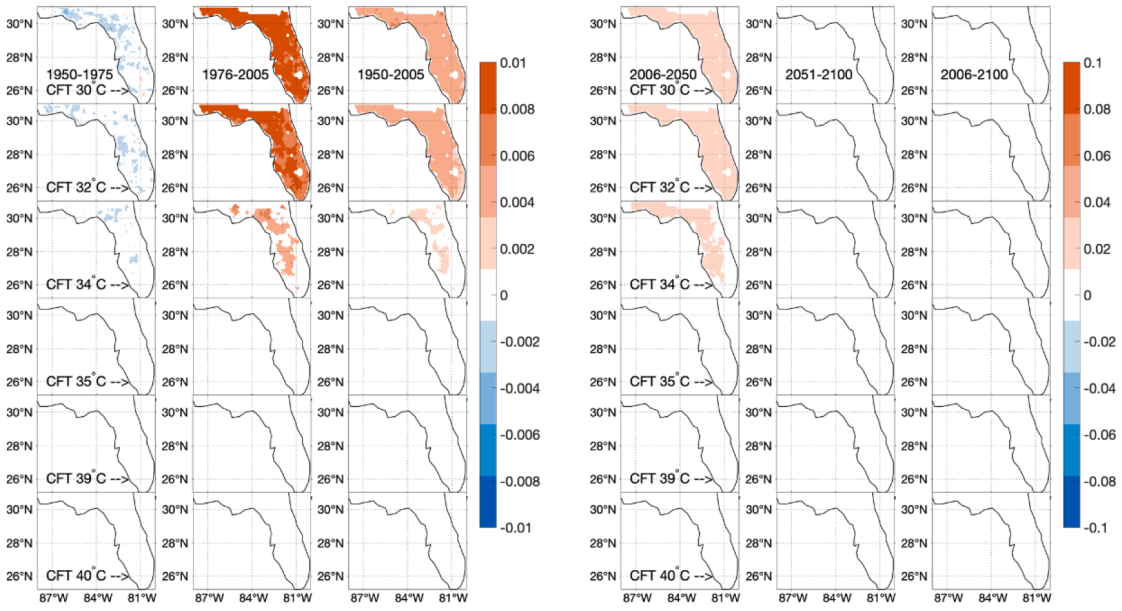

Fig. 6. Median intensity plots for historical simulation in the first three columns (1950–1975; 1976–2005 and 1950–2005) and RCP 8.5 in the last three columns (2006–2050; 2051–2100 and 2006–2100). Statistical significance was tested with a *t*-test with a confidence interval of 90%.

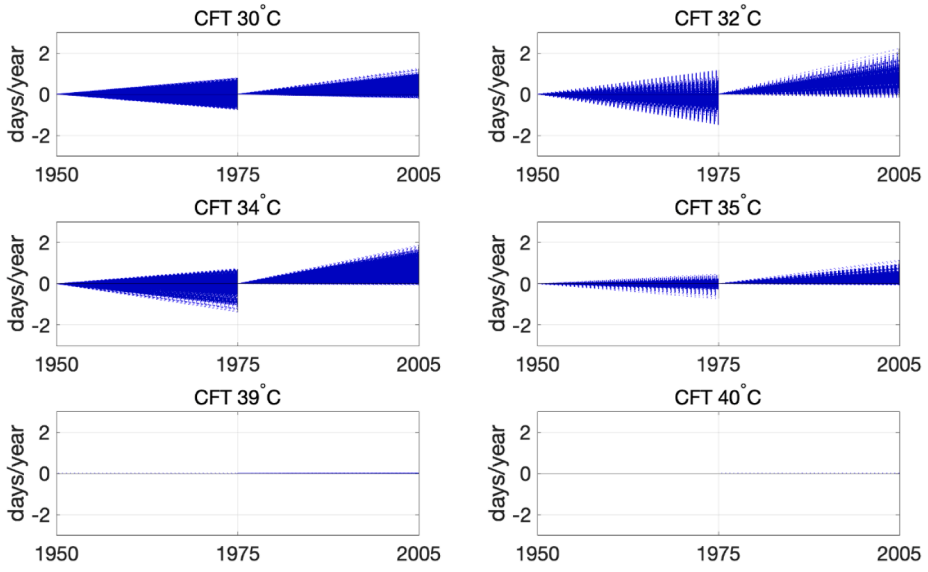

Fig. 7. Funnel plot showing the annual mean frequency from 1950 to 2005 for each CFTs. Significant trend values were shown in the day/year tested with a *t*-test ($\alpha = 0.05$).

period. CFT 32 °C, shows the changes in the range from −1.5 to 1.16 day/year and its maximum cone limit to 2.21 day/year for 1976–2005 time period. For 34 °C, the trends were observed from −1.36 to 0.73 day/year for 1950 to 1975 time period, which is increasing to 1.86 days/year for the 1976–2005 time period. Similarly, for 35 °C, the trends were observed from −0.72 to 0.46 day/year and increasing to 1.14 day/year for the 1976–2005 time period. For 39 °C and 40 °C, no trends were observed during the 1950–2005 period. All the above threshold indicates the warming in the upper and lower threshold of the cone.

Likewise, for RCP 8.5, funnel scenario (Fig. 8), trends are showing only positive slope values with a more significant number of days crossing the temperature thresholds as time period goes in the future. CFT 30 °C, the trends were showing only positive values ranged from 0.09 to 1.30 day/ year for 2006–2050. However, both negative and positive trends for the 2050–2100 time period varies from −2.1 to 1.94 day/year, negative projection show only for few grid points or model only. For CFT 32 °C, the trends were observed positive for 2006–2050 ranged from 0.08 to 2.25 day/year and observed negative and positive trends for 2050–2100 ranged from −1.49 to 2.17 day/year. As the threshold increases, the minimum trend varies decreases for other thresholds, showing the number of days with Tmax were higher than CFTs. For 35 °C, the trends were observed positive, i.e., 0.07 to 2.52 day/year for 2006 to 2050 and −0.60 to 2.94 day/year for the 2051–2100 time period. But for 39 °C, the trend was observed less for 2006 to 2050 ranged from 0 to 0.13 day/year and increase to 2.6 day/ year for2050 to 2100 time period. Similarly, for 40 °C, the trends were observed again less for 2006 to 2050 ranged from 0 to 0.04 and increase up to 1.85 day/ year for the 2051–2100 time period. All ranges in the funnel scenario plots clearly explain that under the RCP 8.5, the number of days with Tmax were more significant under the 32 °C and 34 °C.

For the intensity scenario funnel plot, plots were observed to see the

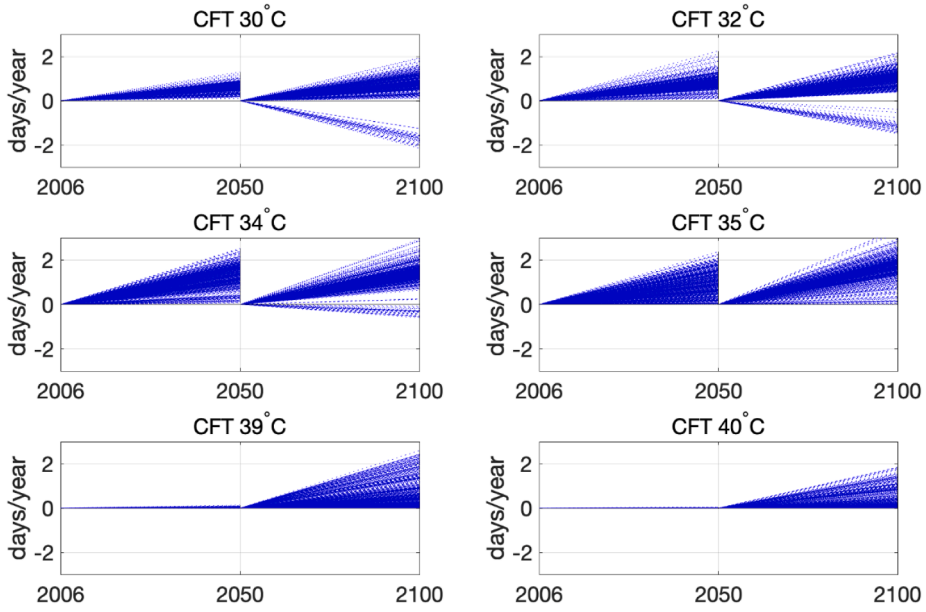

Fig. 8. Funnel plot showing the annual mean frequency from 2006 to 2100 for each CFTs. Significant trend values were shown in the day/year tested with a *t*-test ($\alpha = 0.05$).

increase in the average temperature above the CFTs. As shown in Fig. 9, threshold 30 °C shows trends ranged from −0.02 to 0.02 °C for the 1950–1975 time period and which increased upto 0.04 °C for the 1976–2005 time period.

For 32 °C, the trends were again observed from −0.02 to 0.02 °C for the 1950–1975 time period and which increased up to 0.03 °C for the 1976–2005 time period. Similarly, for 34 °C the trends were observed from 0.01 to 0.02 °C for the 1950–1975 time period and which increased up to 0.02 °C for the 1976–2005 time period. No trends were observed for the 35 °C, 39 °C and 40 °C threshold since there were no events (Tmax) more than CFTs.

Likewise, for RCP 8.5 in Fig. 10, the trends were only showing positive values, which means there was more average temperature higher than CFTs. For 30 °C, the trends were observed from −0.001 to 0.001 °C for the 2006–2050 time period and which increased from 0.012 to 0.06 °C for the 2051–2100 time period. For 32 °C, the trends were observed from 0 to 0.03 °C for the 2006–2050 time period and which increased from 0.006 to 0.06 °C for the 2051–2100 time period. For 34 °C, the trends were observed from −0.002 to 0.03 °C for the 2006–2050 time period and which increased from 0.006 to 0.06 °C for the 2051–2100 time period. For 35 °C, the trends were observed from −0.005 to 0.02 °C for the 2006–2050 time period and which increased from 0.006 to 0.06 °C for the 2051–2100 time period. No trends were observed for the 39 °C and 40 °C threshold since there were no events (Tmax) more than CFTs.

3.5. Failure temperatures and its impact on different crops

This section discusses the effects of various extreme high temperatures on different crops, observed from studies conducted using multiple methods such as controlled environment chambers, field studies, and crop model simulations. Some definitions used in this section were

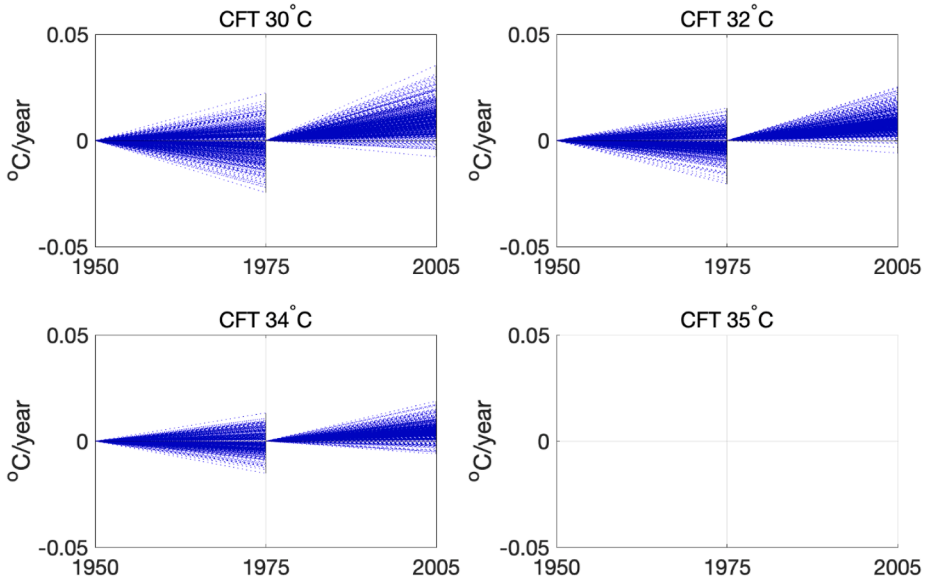

Fig. 9. Funnel plot showing the annual mean intensity from 1950 to 2005 for each CFTs. Significant trend values were shown in the day/year tested with a *t*-test ($\alpha = 0.05$).

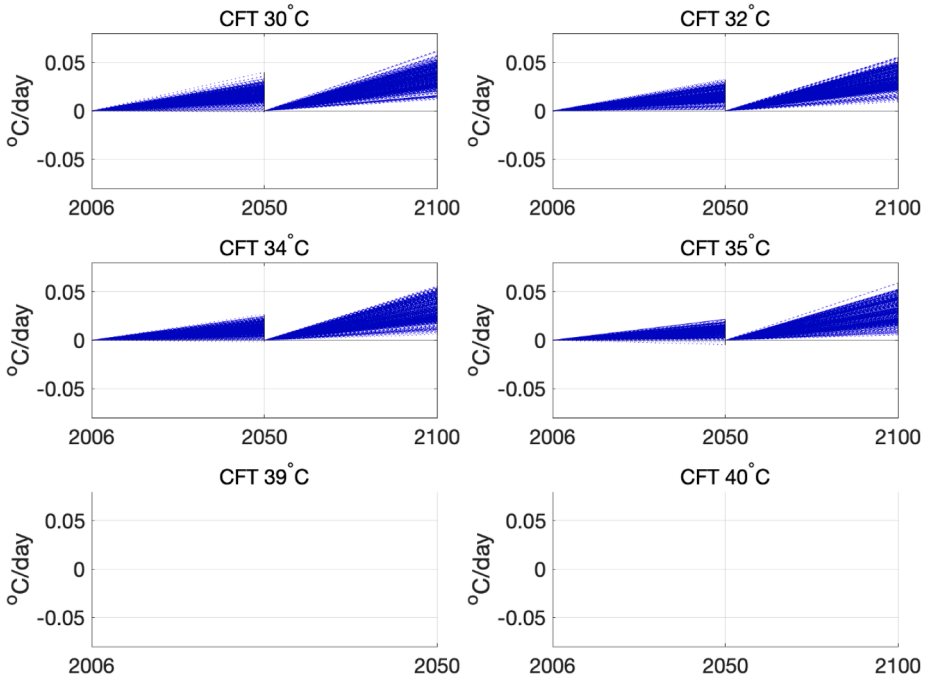

Fig. 10. Funnel plot showing the annual mean intensity from 2006 to 2100 for each CFTs. Significant trend values were shown in the day/year tested with a *t*-test ($\alpha = 0.05$).

harvest index [the ratio of the harvested product (lint and seed for cotton, grain for soybean, maize, peanut, bean) to the above-ground plant dry weight or biomass (stems, leaves, and fruit)]. In this section, the format 44/34 °C describes daytime maximum/nighttime minimum temperature regimes. The summary of the impacts on different crops from crop failure temperature is in Table S2.

In this study, the CFT for the cotton crop is 39 °C. Temperature is one of the most important environmental factors affecting plant reproductive processes (pollen germination, pollen tube growth, and fruit (boll)-set (Kakani et al., 2005). Some of the impacts in cotton due to several temperature ranges include (1) zero boll yield at 40/32 °C maximum/nighttime minimum temperature regimes (35 °C mean) (Hatfield et al., 2008); (2) temperatures greater than 29 °C reduces pollen tube elongation in an experimental filed in Missisippi (Fig. 2 in Kakani et al. 2005); (3) with 25-26 °C and 28 °C temperatures, the maximum growth rate per boll and highest boll harvest index occurred, declining at higher temperatures, while reaching zero boll harvest index at 33–34 °C(Hatfield et al., 2008); (4) mean temperature higher than 30 °C, percent boll set, boll number, boll filling period, rate of boll growth, boll size, and yield decreased under ambient and elevated $C0_2$ (Reddy et al., 2005); (5) instantaneous air temperature above 32 °C reduces pollen viability (Hatfield et al., 2008); (6) from field studies in Missisippi, (Pettigrew, 2008) observed that for two cotton genotypes with 1 °C increase than current temperatures resulted in 10% lower lint yield, 6% decrease in boll mass and 7% less seed in the bolls than the control; (7) cotton yield projected using a quadratic equation from its optimum at 25 °C to its failure temperature of 35 °C, then a 1.2 °C increase from 26.7 °C to 27.9 °C would decrease of 5.7% (Hatfield et al., 2008); (8) in a study from China, using models (CMIP5 and RZWQM2 cotton crop model) and RCP 8.5 scenario, during 2061–2080 predicted yield decreased by 0.28 Mg ha^{-1} (6.5%), with a maximum reduction of 0.73 Mg ha^{-1} (17.3%) for the MPI-ESM-LR CM (Chen et al., 2019); (9) a 4–17% decrease in seed cotton yield (CO_2 at 380 ppm) was observed in DSSAT model and three regional climate models for A2 scenarios for CMIP3 simulations applied to Texas; (10) high temperatures (1.8 °C and 4 °C during 2021–2050 and 2071–2100) in some regions in Greece appeared to be less favourable to seedcotton yield by this change when they used a combination of eight climate models and AquaCrop crop model (Voloudakis et al., 2015); (11) temperature increase by 3.56–4.55 °C (projected under RCP8.5) resulted in decrease in seed cotton yield by 6.5% for 2061–2080 (Chen et al., 2019); (12) using combinations of several CMIP5 models and RZWQM2 crop model, showed an 10% net cotton yield loss for RCP 8.5 in 2080 when compared to baseline climate (1960–2015) which superseded the fertilization effect of CO2 in cotton growth (Anapalli et al., 2016).

The CFT in sorghum is 39C in this study. The pollen viability and pollen numbers are primary reasons for the failure of grain set, and grain yield in sorghum at elevated temperatures with no panicles emerged at 44/34 °C grown under sunlit controlled experiments (Boote et al., 2018). Some of the other impacts in cotton due to several temperature ranges include: High temperature (≥36/26 °C) significantly lowered seed set, seed number, seed size, seed-filling duration, and seed yields; temperatures 36/26 °C to 44/34 °C, significantly reducted leaf photosynthetic rates, while at 44/34 °C, panicle exertion was completely inhibited were some observations from a study from India using InfoCrop-SORGHUM simulation model (Srivastava et al., 2010). This is supported by controlled environments for grain-sorghum cultivar DeKalb 28E, where temperatures above 36/26 °C significantly reduced pollen production, pollen viability, seed-set, seed yield, and harvest index (Prasad et al., 2006) and falling to zero at 40/30 °C (Hatfield et al., 2008) or 35 °C mean temperature (Boote et al., 2018). The temperature of 40/30 °C delayed panicle exertion by ~30 days; 40/30 °C and 44/34 °C inhibited panicle emergence (Prasad et al., 2006). In another study, the elevated temperature during the time to panicle emergence increased from 41 days after sowing (DAS) at 32/22 °C to 60 days at 40/30 °C temperature with only 10% occurrence of panicle emergence (Boote et al., 2018). Finally, from global-scale climate-yield relationships, an 8.4% reduction in the mean sorghum yield for every 1 °C increase in temperature was observed (Hatfield et al., 2008).

Maize is one of the most studied crops for temperature response (Hatfield et al., 2011). The CFT in maize is 35 °C in this study. In maize, the kernel number is a crucial yield component to determine the final maize grain yield (Lizaso et al., 2018). Some of the impacts in maize during multiple temperature ranges include: (1) An 7% maize yield decrease was predicted per 1 °C increase relative to mean temperature globally and a 6% yield reduction with average temperature > 30 °C

each day was predicted for dryland maize in the United States (Rotundo et al., 2019); (2) simulated maize yields in the central Corn Belt decreased 5 to 8% per 2 °C temperature increase which leads to the prediction that a temperature rise of 0.8 °C over the next 30 yr in the Midwest could decrease grain yields by 2 to 3% (Hatfield et al., 2008); (3) at global scale from climate-yield relationships during 1961 to 2002, 8.3% decrease was found per 1 °C increase in temperature (Hatfield et al., 2008).

The CFT in peanut is 39 to 40 °C in this study. Some of the impacts in peanut during multiple temperature ranges include: (1) at 44/34 °C no seed growth was obtained, and no seeds were formed in the tagged flowers (Vara Prasad et al., 2003); (2) The above failure temperature for zero peanut yield occurs at 40 °C (Boote et al., 2018); (3) at 44/34 °C and 45/35 °C a 90% decrease in yield at ambient CO_2 and a zero seed harvest index respectively were observed (Vara Prasad et al., 2003); (4) peanut produced zero yields at 44/34 °C (Boote et al., 2018); (5) in Henry county (Alabama, US), yields reduced by 11.7% and 8.6% per 1 °C rise in mean temperature during the growing season under rainfed conditions, and under irrigated conditions respectively (Ruane et al., 2014); (6) From controlled environment growth chambers, at ambient CO2, seed yield decreased by 14% and 90% and seed harvest index reduced from 0.41 to 0.05 as temperature increased from 32/22 °C to 44/34 °C, respectively under several CO_2. Additionally, pollen viability decreased to 68% at 40/30 °C to zero at 44/34 °C, while seed-set reduced to 50% at 40/30 °C and zero at 44/34 °C under both ambient and elevated CO2 (Vara Prasad et al., 2003).

Peanut's and soybean's CFT is 39–40 °C (Boote et al., 2018). The yield response to temperature in both these crops is due to functions affecting the rate of pollination, seed-set (pod addition), and individual seed growth (Boote et al., 2018). Some of the impacts in soybean during multiple temperature ranges include: (1) pod number lowered and sharply as sharply decreased as temperature exceeded at 40/30 °C (Pan, 1996); (2) a decline in yield, seed size, and harvest index when temperature increases, reaching zero yields and zero seed harvest index at 39 °C (Hatfield et al., 2008); (3) yield decreased at temperatures above 36/26 °C under sunlit controlled environment chambers (Thomas, 2001); (4) pollen viability of soybean decreased from temperatures > 30 °C with a long decline slope to failure at 47 °C; reduced pollen production by 34%, pollen germination by 56%, and pollen tube elongation by 33% (Hatfield et al., 2008); (5) the weight per seed decreased as temperature increased from 28/18 °C to 44/34 °C regardless of [CO_2] (Thomas, 2001).

In this study, the CFT for the tomato crop is 30 °C. Tomato industry is one of the most globalized and advanced horticultural sectors, with an increase of about 300% global annual production during the last four decades (Pathak and Stoddard, 2018). Some of the impacts in tomato during multiple temperature ranges include: (1) with increase in mean daily temperature from 25 to 29 °C, yield related characteristics, including seeds per fruit, declined sharply., with temperatures > 25 °C (30/21 °C) reduced fruit production (Peet et al., 1998); (2) Rate of fruit addition (fruit-set, from pollination) progressively fails as temperature reaches 32 °C beyond optimum temperature of 26 °C (Adams, 2001; Hatfield et al., 2008); (3) there was a reduction of 90% in the number of fruits per plant at 32/26 °C day/night (29 °C mean) when compared to those in 28/22 °C (25 °C mean) (Peet et al., 1998); (5) assuming an optimum temperature and failure temperatures for yield of 23.5 °C and 30 °C, respectively, yield was projected to decrease 12.6% for 1.2 °C rise above optimum in a non-linear yield response (Hatfield et al., 2008); (6) at 32/26 °C temperature for 0–15 days before anthesis the set fruit failed due to disruption of anther components (Sato et al., 2002); (7) temperatures > 35 °C caused poor pollination and flower abortion (Hartz et al., 2008); (8) increased heat during the blooming period reduces yield (Pathak and Stoddard, 2018); (9) at high temperatures, tomato yellow leaf curl virus infection occurs most frequently, enhanced by the presence of whiteflies (B. tabaci), infected transplants and weedy fields with many alternative hosts. Besides, the insect vector (B. tabaci) also prefers high temperatures (Ramos et al., 2019); (10) pollen sterility occurs at 32 °C, while at temperatures from 28/22 °C to 32/26 °C decreased fruit set with significantly higher decrease with > 35 °C, while pollen sterility occurs at 32 °C (Shah Chishti et al., 2019).

In this study, the CFT for the bean crop is 30 °C. A 5% yield declines/decade was observed on harvested, and 12% yield declines respectively on the sown area at an annual and national scales (Sanders et al., 2019). The red kidney bean crop showed zero yields as temperature increased to 37/27 °C (32 °C mean)(Hatfield et al., 2008). When flower buds were exposed to 32/27 °C during the 6–12 days before anthesis resulted in reduced fruit-set and at anthesis, caused by non-viable pollen, failure of anther dehiscence, and reduced pollen tube growth (Gross and Kigel, 1994). Bean yield will likely reduce ~ 7.2% and 8.6% per 1 °C and 1.2 °C, respectively, for temperature rise > 23 °C (Hatfield et al., 2008). Model results show that bean is highly temperature-sensitive, with a decline of 21% yield relative to mean values per °C (Gourdji et al., 2015).

3.6. Adaptation strategies for CFTs to reduce or positive impacts

This section discusses the various adaptation strategies discussed in the literature to reduce the adverse effects of extremely high temperatures changes in three ways (Fig. 11, Table S3, and explained in text form). The plant's ability to withstand these stresses greatly varies from species to species is improved by adopting the genetic approaches or by inducing the stress resistance (Fahad et al., 2017). Adaptation is also considered as one of the policy responses to the impacts of drivers and pressures (Smit and Skinner, 2002). It can involve decision-making by stakeholders and producers. Implementing adaptation options reduce vulnerability, improve resilience to future changes, and higher potential for well-being (Lim et al., 2005).

Some definitions used in this section are adaptation strategies, which are defined as the general plan or some action for addressing the impact of climate change, including climate variability and extremes, which includes various policies and measures with a specific objective to reduce vulnerability (Biesbroek et al., 2010). The term stakeholders encompass a spectrum of professions and are broadly used to ensure inclusivity as to whom can utilize the methods/results used in this study.

Adaptation strategies for changes in CFTs can be described under three levels of adaptation strategies, i.e., (1) Incremental adaptation, (2) System adaptation, and (3) Transformation adaptation. Incremental plans are the practices and technologies with minor changes (such as changing planting dates) within existing fields; System adaptation strategies which are the significant changes in existing agriculture fields (such as precision agriculture) and; Transformational strategy are the ones with robust change (such as land-use change) in a new area rather than the existing one (Anandhi, 2016). There could be an increase in intricacy, cost, and risks in action while moving from incremental to transformational change (Howden et al., 2007; Kates et al., 2012).

Each level of the adaptation strategies has approaches to reduce the impact of CFTs and to utilize the benefits of CFTs for different crops, as shown in Fig. 11.

Different studies have been done on different crop adaptation strategies being impacted by high crop temperatures. Some of the adaptation strategies observed in literature are (1) (Morales et al., 2003) observed preconditioning as an adaptation strategy. The preconditioning was to expose the 20-day old tomato plant to 4 day each of 30/23 and 35/28 temperatures to combat the heat stress because they had better performances due to better osmotic and stomatal adjustment; (2) (Ventrella et al., 2012) suggested adaptation strategies such as an increase in the frequency of irrigation (i.e., start the automatic irrigation when soil reached 40 and 60% of available crop water) and nitrogen fertilization showed a positive effect in minimizing the negative impacts of climate change on the productivity of tomato cultivate in southern Italy. They also observed these strategies for a temperature change of around 5 °C; (3) (Fahad et al., 2017) suggested preconditioning of plants

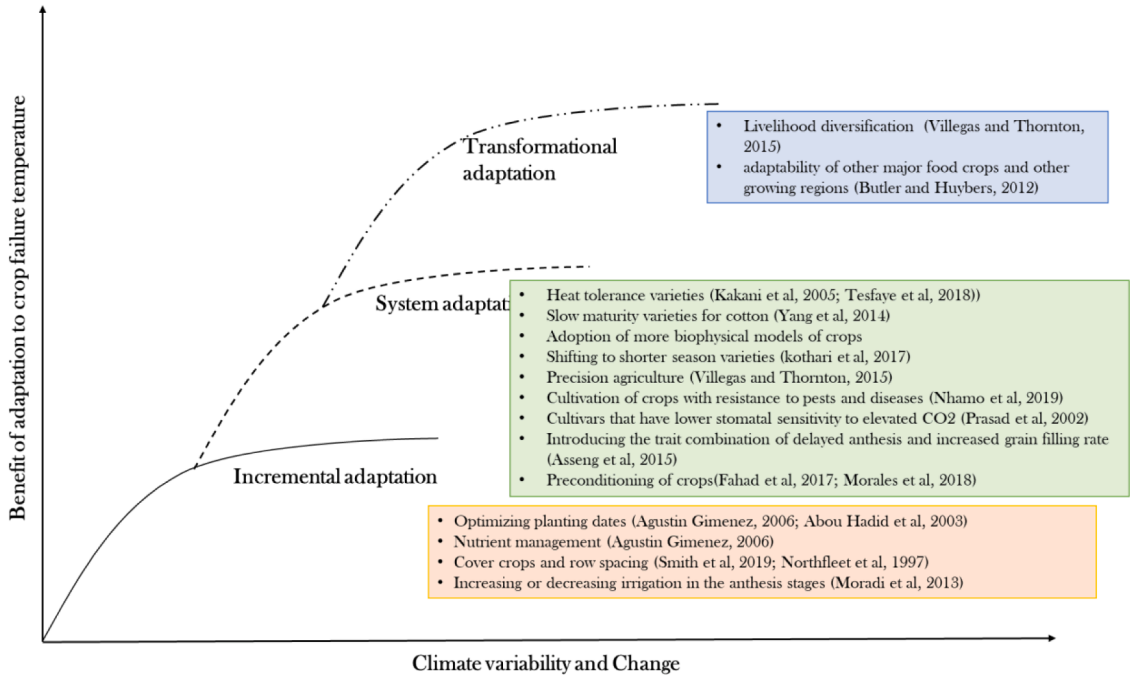

Fig. 11. Adaptation Strategies showing the three levels of adaptation with different approaches that reduce the impact and benefits from effects.

through pre-sowing hydration of the seed in such a way that the germination metabolism is initiated. Still, the emergence of the radicle is avoided proved very useful to combat heat stress. For example, pre-sowing the seeds of pearl millet when exposed to a higher temperature (42 °C) resulted in better performance; (4) (Mauget et al., 2019) suggested early planting of cotton to combat heat stress. They observed this provides additional growing degree days from May planting can substantially increase lint yields relative to June planting, while minimizing a cotton crop's later exposure to cooling hours; (5) (Kakani et al., 2005) observed identification of cotton cultivars with high-temperature tolerance would be beneficial in high-temperature environments with > 30 °C during flowering to improve boll retention and yield in cotton; (6)

((Moradi et al., 2013) suggested, in general for Maize in Iran, an earlier planting date (1 May from May 10 and 20) and changing irrigation intervals in the anthesis stage as adaptation strategies; (7) (Asseng et al., 2019) observed genotypes with a trait of an extended growing period to delay anthesis, combined with a character with a

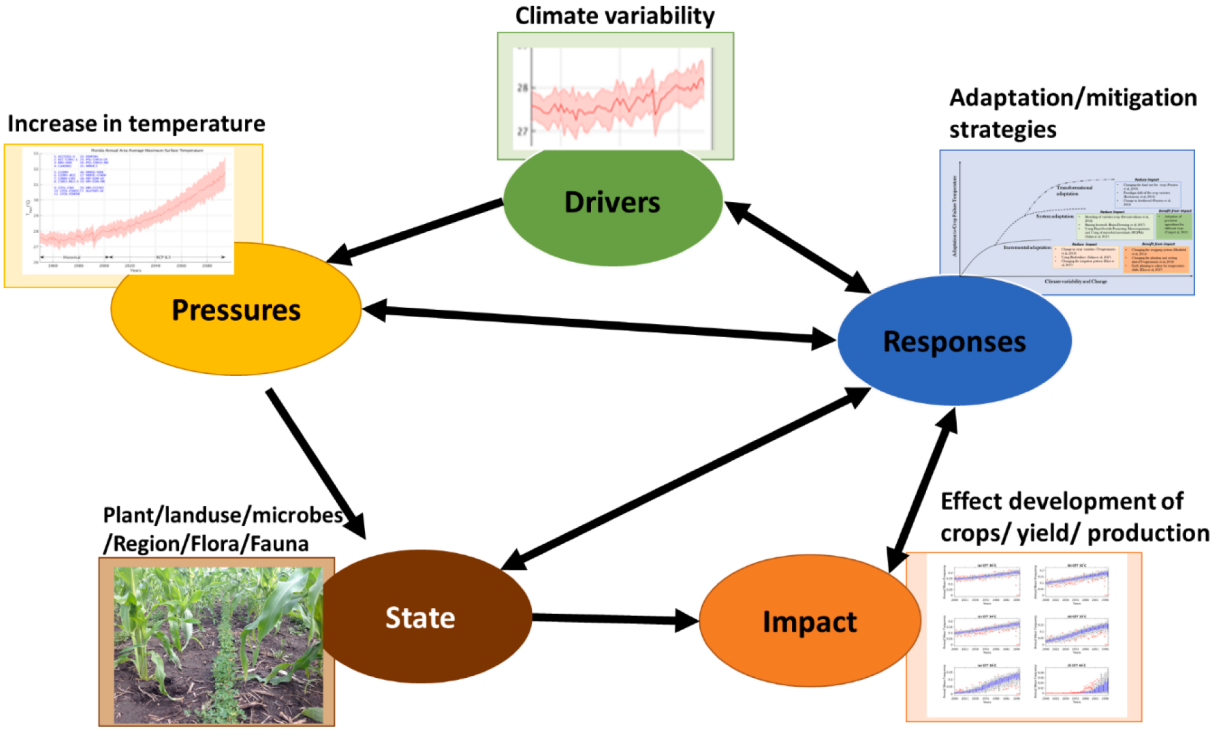

Fig. 12. DPSIR framework for the crop failure temperature.

higher rate of grain filling were effective in countering some of the yield declines occurring in non-adapted cultivars when grown in warmer locations or during a warmer part of a season. They suggested this can improve global yield by 9.6% by 2050; (8) (Boomiraj et al., 2010) synthesized several quantitative strategies for multiple crops from 2002 to 2006.

3.7. Development of causal chain/ loop to develop adaptation strategies

The DPSIR framework is used to describe the issue of crop vulnerability in this study. The changes in temperature (drivers) impact the crops as one indicator, i.e., crop failure temperature (CFT) (Pressure) and changes the condition of the environment for plants and soil, which are heat stresses (State). The change in the state have significant impacts on the state as the decline in crop productivity, plant death, etc. (Impact) and finally measures to reduce the vulnerability or impact which can be changed in planting dates, modifying the crop genetics (responses to develop adaptation strategies) which would help stakeholders and managers as shown in Fig. 12.

This DPSIR was further made complex to develop the causal chain and loop to show the cause-effect relationship till the end and to understand the feedback mechanism. This causal loop also maps the structure of driver, pressures, which changes the state condition, giving direction to impacts and adding responses, which therefore leads to being one driver or pressure. It was explained with the help of examples for CFT 30 °C and CFT 35 °C based on literature review. In Fig. 12, two causal loops have been developed (a) CFT 30 °C and (b)CFT 35 °C, which has their multi-level impacts and responses. For example, in Fig. 13a, the increase in temperature results in an increase in the number of days (frequency) and mean temperature above crop failure temperatures (intensity) 30 °C) and increases the probability of changing the state of soil and crop, i.e., soil moisture and heat stresses tomato. The change in this state will eventually make the tomato plant dead and decrease productivity and increase soil erosion. Thereby, responses will help in

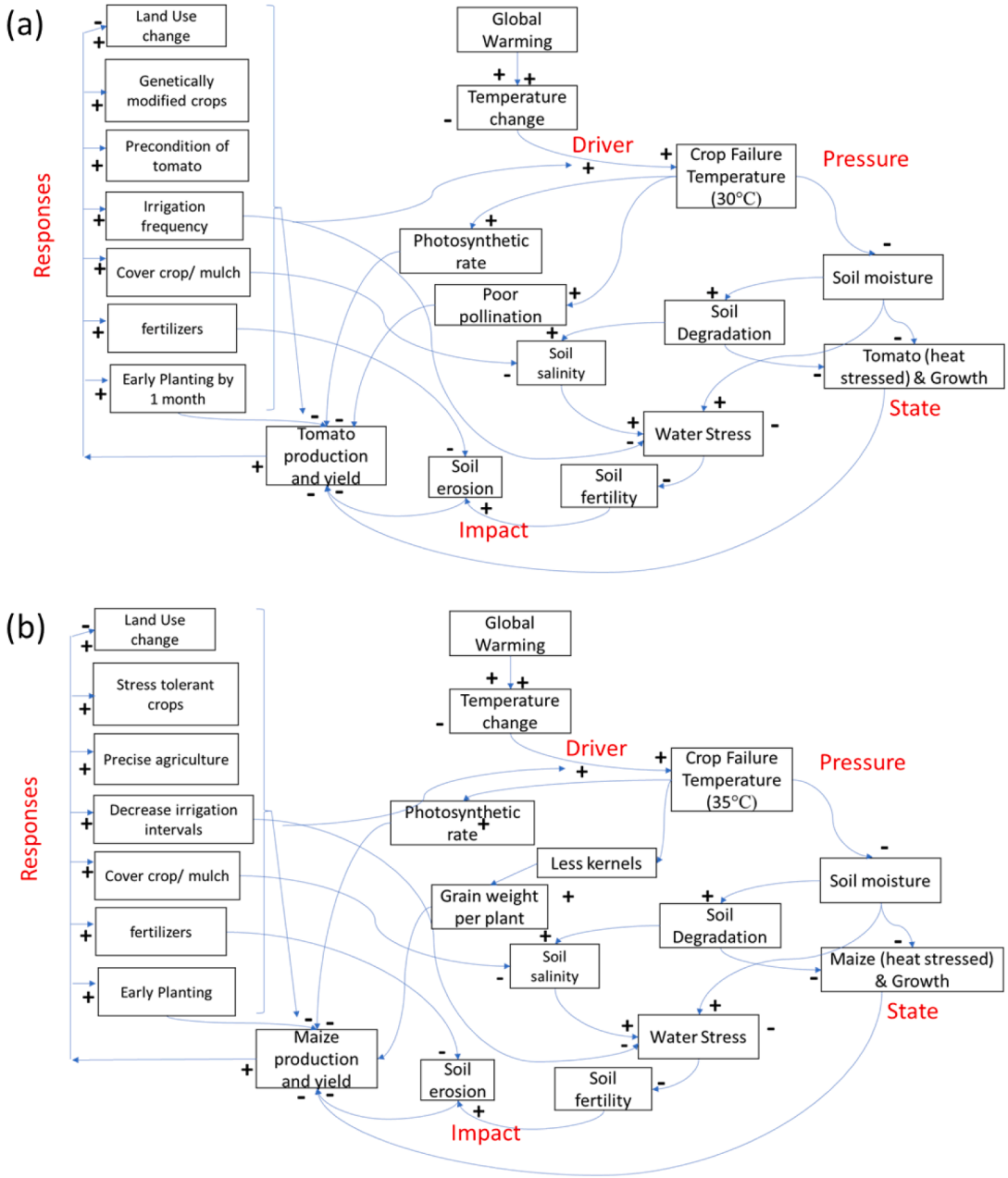

Fig. 13. The causal chain and loops development with the help of the DPSIR framework for a) CFT at 30 °C and b) CFT 35 °C.

easing the harsh impacts by early planting of tomato plant by one month, using cover cropping method and mulch, increasing the frequency of irrigation, growing the genetically modified crop varieties or changing the land use for tomato plants will eventually help policymakers and stakeholder to use responses for their purpose.

Similarly Fig. 13b shows the increase in change in temperature results in the rise in temperature results in an increase in the number of days (frequency) and mean temperature above crop failure temperatures (intensity) (35 °C) and increases the probability to change the state of soil and crop, i.e., soil moisture and heat stresses maize. The change in this state will eventually make the maize crop dead and decrease the productivity with less percentage of the kernel or less percentage of grain weight per plant and increase the soil erosion. Thereby, responses will help in reducing the impact by various strategies like early planting of a maize plant by one month, using cover cropping method and mulch, increasing the frequency of irrigation, increasing the genetically modified crop varieties, or changing the land use for tomato plants will eventually help policymakers and stakeholder to use responses for their purpose Adaptation strategies in this study provides better insight which highlights the complexity and considered a government policy response in agriculture, as it involves decision-making by stakeholders and producers (Smit and Skinner, 2002) which is further discussed.

4. Discussion

In this study, CFT was demonstrated as a useful ecosystem indicator for changing diurnal temperatures and their impact on crops in Florida. CFT was also used to develop the causal chain and loop using the DPSIR framework to provide quantitative values. The usefulness of CFT was demonstrated using observations and CMIP5 model simulations for historical and future scenarios. From the scenario funnel plots, it is evident that frequency was found to be increasing at the rate of 2 days/year. For intensity, it was found in the range of 0.02 to 0.04 °C from 2006 to 2100 that will help in understanding the big picture of changing trends, the impacts of it and addressing the responses. The causal chain and loop were also developed to understand the complex structure and feedback mechanism for CFT at 30 °C and 35 °C. This also addresses that the causal chain and loop will finally help in bridging the gap between climate and crop to discuss the adaptation strategies if the impacts are known.

4.1. Contribution of technological diffusion and policy measures for sustainable development

Contribution of technological diffusion during the last few years have been put forward to combat the problem, mainly targeting the unsustainable urban development and cleaner production (Aldieri et al., 2019). These include empirical shreds of evidence that strict policies, such as carbon tax, promote corporate innovation and knowledge sharing, which enhance firm productivity and financial value. Adopting new development paradigms to make cities more sustainable, resilient, and smarter—e.g., smart city and intelligent urbanism movements (Aldieri et al., 2019, 2020) and incentivizing green technology and cleaner industrial development. Environmental innovation through technological diffusion has given importance since it can be useful in combating the problems in agriculture and help in the modernization of clean and green earth (Aldieri et al., 2019). Technological diffusion focuses predominantly on the invention and innovation, or science and R&D like genome practices (Gupta et al., 2020) or new varieties of crops that confer tolerance to drought and heat, tolerance to salinity and early maturation to shorten the growing season and reduce farmers' exposure to the risk of extreme weather events; adoption of modern irrigation techniques that contribute a change in productivity growth (Chatzimichael et al., 2020) like the adoption of wet-dry irrigation technologies (Alauddin et al., 2020), adoption of climate-smart farm practices (Nowak, 1987; Pagliacci et al., 2020; Shahzad and Abdulai, 2020).

Policy measures for sustainability development also played a crucial role in agriculture that is affected by climate variability. Implementation of technological diffusion through policy mix is critical to achieving sustainable economic growth. Hence, adopting climate-smart agriculture through i) improving the design of financially supported voluntary schemes and the related tools of information provided to farmers; and ii) complementing them with proactive information-based regulations (Pagliacci et al., 2020) helps in improving the vulnerability. Significant policy implications also include information diffusion about the CSA through farmers' education and training for widespread adoption and diffusion of water-saving technologies, a substantial strengthening of institutional support services, scientific research, and rethinking of the cropping-mix (Alauddin et al., 2020). Lack of awareness for the technological diffusion at the farmer's level is one of the limiting factors which can be reduced by making an effort at the farmer's level to adopt the technology. For progress on implementing adaptations to climate change in agriculture, there is a need to better understand the relationship between potential adaptation options and existing farm-level and government decision-making processes and risk management frameworks (Smit and Skinner, 2002). Innovations in microfinance generally and in micro-insurance products specifically may aid farmers' capacity to adapt to climate change, especially in settings that will experience more significant variability and more frequent extreme events (Lybbert and Sumner, 2012).

In our study, technological diffusion is the adoption of adaptation strategies for the crops that are impacted by the high temperature. For example, the adoption of genetically improved crops, adopting conservation agriculture, using water-saving technologies, etc. not only reduces the effects on crops but also increase productivity and benefits in an area. This study is very important because the knowledge flows through adaptation strategies for clean technologies by stakeholders and managers, which not only help domestically but nationally through Intra sectorial spillovers. Knowing the impacts of climate on crops helps in adopting adaptation strategies at different levels, i.e., 1) Incremental adaptation, (2) System adaptation, and (3) Transformation adaptation will help stakeholders and farmers, etc. for better understanding of technological diffusion in agricultural land. Moreover, the DPSIR also provides a practical methodology, i.e., causal chain and loop that can effectively capture the entire range of causes and effects and the interrelations between indicators and thereby will help the environment for a better future world.

5. Conclusion

This study is unique because the crop failure temperature used 21 CMIP5 models during historical (1950–2005) and future RCP 8.5 (2006–2100. Then they were combined with quantitative impacts and adaptation strategies from published literature with frequency and intensity trends in CFTs (data analyzed) to develop causal chains/loops using the DPSIR framework. The combination of synthesizes and data analysis to create causal chains/loops would improve the linkage between climate impacts and adaptation research for planning and management studies so stakeholders can use this study for their practices and work.

CRediT authorship contribution statement

Anjali Sharma: Validation, Writing - original draft, Visualization. **Aavudai Anandhi:** Supervision, Conceptualization, Funding acquisition, Project administration.

Declaration of Competing Interest

The authors declare that they have no known competing financial interests or personal relationships that could have appeared to influence the work reported in this paper.

Acknowledgements

This material is based upon work partially supported by the USDA-NIFA capacity building grant 2017-38821-26405, USDA-NIFA Evans-Allen Project, Grant 11979180/2016-01711, USDA-NIFA grant No. 2018-68002-27920 and National Science Foundation under Grant No. 1735235 awarded as part of the National Science Foundation Research Traineeship. Ms. Goodman's support with the methodology is acknowledged. National institute for food and agriculture, United States.

Appendix A. Supplementary data

Supplementary data to this article can be found online at https://doi.org/10.1016/j.ecolind.2020.107064.

References

Adams, S., 2001. Effect of temperature on the growth and development of tomato fruits. Ann. Botany 88, 869–877.
Adhikari, P., Ale, S., Bordovsky, J.P., Thorp, K.R., Modala, N.R., Rajan, N., Barnes, E.M., 2016. Simulating future climate change impacts on seed cotton yield in the Texas High Plains using the CSM-CROPGRO-Cotton model. Agric. Water Manage. 164, 317–330.
Alauddin, M., Rashid Sarker, M.A., Islam, Z., Tisdell, C., 2020. Adoption of alternate wetting and drying (AWD) irrigation as a water-saving technology in Bangladesh: economic and environmental considerations. Land Use Policy 91.
Aldieri, L., Carlucci, F., Vinci, C.P., Yigitcanlar, T., 2019. Environmental innovation, knowledge spillovers and policy implications: a systematic review of the economic effects literature. J. Cleaner Prod. 239, 118051.
Aldieri, L., Grafström, J., Sundström, K., Vinci, C.P., 2020. Wind power and job creation. Sustainability 12–45.
Anandhi, A., 2016. Growing degree days – ecosystem indicator for changing diurnal temperatures and their impact on corn growth stages in Kansas. Ecol. Ind. 61, 149–158.
Anandhi, A., Bentley, C., 2018. Predicted 21st century climate variability in southeastern U.S. using downscaled CMIP5 and meta-analysis. CATENA 170, 409–420.
Anandhi, A., Blocksome, C.E., 2017. Developing adaptation strategies using an agroecosystem indicator: variability in crop failure temperatures. Ecol. Ind. 76, 30–41.
Anandhi, A., Kannan, N., 2018. Vulnerability assessment of water resources – translating a theoretical concept to an operational framework using systems thinking approach in a changing climate: case study in Ogallala Aquifer. J. Hydrol. 557.
Anandhi, A., Omani, N., Chaubey, I., Horton, R., Bader, D.A., Nanjundiah, R.S., 2016a. Synthetic scenarios from CMIP5 model simulations for climate change impact assessments in managed ecosystems and water resources: case study in South Asian Countries. Trans. ASABE 59, 1715–1731.
Anandhi, A., Steiner, J.L., Bailey, N., 2016b. A system's approach to assess the exposure of agricultural production to climate change and variability. Clim. Change 136, 647–659.
Anandhi, A., Sharma, A., Sylvester, S., 2018. Can meta-analysis be used as a decision-making tool for developing scenarios and causal chains in eco-hydrological systems? Case study in Florida: can meta-analysis be used as a decision making tool in eco-hydrological systems? Ecohydrology 11, e1997.
Anapalli, S., Fisher, D., Reddy, K., Pettigrew, W., Sui, R., Ahuja, L., 2016. Vulnerabilities and adapting irrigated and rainfed cotton to climate change in the lower Mississippi Delta Region. Climate 4.
Asseng, S., Martre, P., Maiorano, A., Rotter, R.P., O'Leary, G.J., Fitzgerald, G.J., Girousse, C., Motzo, R., Giunta, F., Babar, M.A., Reynolds, M.P., Kheir, A.M.S., Thorburn, P.J., Waha, K., Ruane, A.C., Aggarwal, P.K., Ahmed, M., Balkovic, J., Basso, B., Biernath, C., Bindi, M., Cammarano, D., Challinor, A.J., De Sanctis, G., Dumont, B., Eyshi Rezaei, E., Fereres, E., Ferrise, R., Garcia-Vila, M., Gayler, S., Gao, Y., Horan, H., Hoogenboom, G., Izaurralde, R.C., Jabloun, M., Jones, C.D., Kassie, B.T., Kersebaum, K.C., Klein, C., Koehler, A.K., Liu, B., Minoli, S., Montesino San Martin, M., Muller, C., Naresh Kumar, S., Nendel, C., Olesen, J.E., Palosuo, T., Porter, J.R., Priesack, E., Ripoche, D., Semenov, M.A., Stockle, C., Stratonovitch, P., Streck, T., Supit, I., Tao, F., Van der Velde, M., Wallach, D., Wang, E., Webber, H., Wolf, J., Xiao, L., Zhang, Z., Zhao, Z., Zhu, Y., Ewert, F., 2019. Climate change impact and adaptation for wheat protein. Glob. Change Biol. 25, 155–173.
Ba, Y., Galik, C., 2019. Polycentric systems and multiscale climate change mitigation and adaptation in the built environment. Rev. Policy Res. 36, 473–496.
Ben-Ari, T., Boé, J., Ciais, P., Lecerf, R., Van der Velde, M., Makowski, D., 2018. Causes and implications of the unforeseen 2016 extreme yield loss in the breadbasket of France. Nat. Commun. 9, 1627.
Bentley, C., Anandhi, A., 2020. Representing driver-response complexity in ecosystems using an improved conceptual model. Ecol. Modell. 1 (437), 109320.
Bhardwaj, A., Misra, V., Mishra, A., Wootten, A., Boyles, R., Bowden, J.H., Terando, A.J., 2018. Downscaling future climate change projections over Puerto Rico using a non-hydrostatic atmospheric model. Clim. Change 147 (1–2), 133–147.
Biesbroek, G.R., Swart, R.J., Carter, T.R., Cowan, C., Henrichs, T., Mela, H., Morecroft, M.D., Rey, D., 2010. Europe adapts to climate change: comparing national adaptation strategies. Global Environ. Change 20, 440–450.
Binder, T., Vox, A., Belyazid, S., Haraldsson, H., Svensson, M., 2004. Developing system dynamics models from causal loop diagrams. In: Proceedings of the 22nd International Conference of the System Dynamic Society, pp. 1–21.
Boomiraj, K., Wani, S.P., Garg, K.K., Aggarwal, P.K., Palanisami, K., 2010. Climate change adaptation strategies for agro-ecosystem–a review. J. Agrometeorol. 12, 145–160.
Boote, K.J., Prasad, V., Allen Jr., L.H., Singh, P., Jones, J.W., 2018. Modeling sensitivity of grain yield to elevated temperature in the DSSAT crop models for peanut, soybean, dry bean, chickpea, sorghum, and millet. Eur. J. Agron. 100, 99–109.
Byjesh, K., Kumar, S.N., Aggarwal, P.K., 2010. Simulating impacts, potential adaptation and vulnerability of maize to climate change in India. Mitig. Adapt. Strateg. Glob. Change 15, 413–431.
Chatzidaki, E., Ventura, F., 2010. Adaptation to climate change and mitigation strategies in cultivated and natural environments. A review. Italian J. Agrometeorol. 3, 21–42.
Chatzimichael, K., Christopoulos, D., Stefanou, S., Tzouvelekas, V., 2020. Irrigation practices, water effectiveness and productivity measurement. Eur. Rev. Agric. Econ. 47, 467–498.
Chen, X., Qi, Z., Gui, D., Gu, Z., Ma, L., Zeng, F., Li, L., 2019. Simulating impacts of climate change on cotton yield and water requirement using RZWQM2. Agric. Water Manage. 222, 231–241.
Cheng, C.H., Nnadi, F., Liou, Y.A., 2015. A regional land use drought index for Florida. Remote Sens. 7 (12), 17149–17167.
Edenhofer, O., 2015. Climate change 2014: mitigation of climate change. 3.
Fahad, S., Bajwa, A.A., Nazir, U., Anjum, S.A., Farooq, A., Zohaib, A., Sadia, S., Nasim, W., Adkins, S., Saud, S., Ihsan, M.Z., Alharby, H., Wu, C., Wang, D., Huang, J., 2017. Crop production under drought and heat stress: plant responses and management options. Front. Plant Sci. 8, 1147.
FDACS, 2017. Florida Agriculture Overview and Statistics - Florida Department of Agriculture & Consumer Services. assessed on October 14, 2020. https://www.fdacs.gov/Agriculture-Industry/Florida-Agriculture-Overview-and-Statistics.
Gourdji, S., Läderach, P., Valle, A.M., Martinez, C.Z., Lobell, D.B., 2015. Historical climate trends, deforestation, and maize and bean yields in Nicaragua. Agric. For. Meteorol. 200, 270–281.
Gross, Y., Kigel, J., 1994. Differential sensitivity to high temperature of stages in the reproductive development of common bean (Phaseolus vulgaris L.). Field Crops Res. 36, 201–212.
Gupta, M., Gerard, M., Padmaja, S.S., Sastry, R.K., 2020. Trends of CRISPR technology development and deployment into Agricultural Production-Consumption Systems. World Patent Inf. 60.
Hall, A.E., 1992. Breeding for Heat Tolerance. Plant Breed. Rev 10, 129–168.
Haraldsson, H.V., 2004. Introduction to System Thinking and Causal Loop Diagrams. Department of Chemical Engineering, Lund University, pp. 3–4.
Hartz, T., Miyao, G., Mickler, J., Lestrange, M., Stoddard, S., Nuñez, J., & Aegerter, B., 2008. Processing tomato production in California.
Hatfield, J.L., Gitelson, A.A., Schepers, J.S., Walthall, C.L., 2008. Application of spectral remote sensing for agronomic decisions. Agron. J. 100. S-117.
Hatfield, J.L., Boote, K.J., Kimball, B.A., Ziska, L.H., Izaurralde, R.C., Ort, D., Thomson, A.M., Wolfe, D., 2011. Climate impacts on agriculture: implications for crop production. Agron. J. 103 (2), 351–370.
Howarth, C., Monasterolo, I., 2016. Understanding barriers to decision making in the UK energy-food-water nexus: the added value of interdisciplinary approaches. Environ. Sci. Policy 61, 53–60.
Howden, S.M., Soussana, J.-F., Tubiello, F.N., Chhetri, N., Dunlop, M., Meinke, H., 2007. Adapting agriculture to climate change. Proc. Natl. Acad. Sci. 104, 19691–19696.
Jarvis, A., Lau, C., Cook, S., Wollenberg, E., Hansen, J., Bonilla, O., Challinor, A., 2011. An integrated adaptation and mitigation framework for developing agricultural research: synergies and trade-offs. Exp. Agric. 47, 185–203.
Kakani, V.G., Reddy, K.R., Koti, S., Wallace, T.P., Prasad, P.V., Reddy, V.R., Zhao, D., 2005. Differences in in vitro pollen germination and pollen tube growth of cotton cultivars in response to high temperature. Ann. Bot. 96, 59–67.
Kates, R.W., Travis, W.R., Wilbanks, T.J., 2012. Transformational adaptation when incremental adaptations to climate change are insufficient. Proc. Natl. Acad. Sci. 109, 7156–7161.
Keairns, D.L., Darton, R.C., Irabien, A., 2016. The energy-water-food nexus. Ann. Rev. Chem. Biomol. Eng. 7, 239–262.
Kothari, K., Ale, S., Bordovsky, J., Hoogenboom, G., Munster, C.L., 2017. Assessment of climate change impacts and evaluation of adaptation strategies for grain sorghum and cotton production in the Texas high plains. AGU Fall Meeting Abstracts.
Lim, B., Spanger-Siegfried, E., Burton, I., Malone, E., & Huq, S., 2005 Adaptation policy frameworks for climate change: developing strategies, policies and measures.
Linster, M. (2003). OECD environmental indicators: Development, measurement and use. Zu finden in http://www.oecd.org/environment/indicators-modelling-outlooks/24993546.pdf [zitiert am 30.03. 2015].
Lizaso, J.I., Ruiz-Ramos, M., Rodríguez, L., Gabaldon-Leal, C., Oliveira, J.A., Lorite, I.J., Sánchez, D., García, E., Rodríguez, A., 2018. Impact of high temperatures in maize: phenology and yield components. Field Crops Res. 216, 129–140.
Lybbert, T.J., Sumner, D.A., 2012. Agricultural technologies for climate change in developing countries: policy options for innovation and technology diffusion. Food Policy 37, 114–123.
Marella, R. L. (1999). Water withdrawals, use, discharge, and trends in Florida, 1995 (Vol. 99, No. 4002). US Department of the Interior, US Geological Survey.
Mauget, S., Ulloa, M., Dever, J., 2019. Planting Date Effects on Cotton Lint Yield and Fiber Quality in the U.S. Southern High Plains. Agriculture 9.

Maurer, E.P., Wood, A.W., Adam, J.C., Lettenmaier, D.P., Nijssen, B., 2002. A long-term hydrologically based dataset of land surface fluxes and states for the conterminous United States. J. Clim. 15 (22), 3237–3251.
Moradi, R., Koocheki, A., Nassiri Mahallati, M., Mansoori, H., 2013. Adaptation strategies for maize cultivation under climate change in Iran: irrigation and planting date management. Mitig. Adapt. Strateg. Glob. Change 18, 265–284.
Morales, D., Rodriguez, P., Dell'Amico, J., Nicolas, E., Torrecillas, A., Sanchez-Blanco, M. J., 2003. High-temperature preconditioning and thermal shock imposition affects water relations, gas exchange and root hydraulic conductivity in tomato. Biol. Plant 46, 203.
Neset, T.-S., Wiréhn, L., Klein, N., Käyhkö, J., Juhola, S., 2019. Maladaptation in Nordic agriculture. Clim. Risk Manage. 23, 78–87.
Ness, B., Anderberg, S., Olsson, L., 2010. Structuring problems in sustainability science: the multi-level DPSIR framework. Geoforum 41, 479–488.
Nhamo, L., Mathcaya, G., Mabhaudhi, T., Nhlengethwa, S., Nhemachena, C., Mpandeli, S., 2019. Cereal Production Trends under Climate Change: Impacts and Adaptation Strategies in Southern Africa. Agriculture 9.
Nie, Y., Avraamidou, S., Xiao, X., Pistikopoulos, E.N., Li, J., Zeng, Y., Song, F., Yu, J., Zhu, M., 2019. A Food-Energy-Water Nexus approach for land use optimization. Sci. Total Environ. 659, 7–19.
Niemeijer, D., de Groot, R.S., 2008. A conceptual framework for selecting environmental indicator sets. Ecol. Ind. 8 (1), 14–25.
Nowak, P.J., 1987. The adoption of agricultural conservation technologies: economic and diffusion explanations. Rural Sociol. 52, 208.
O'connell, D., Walker, B., Abel, N., Grigg, N., 2015. The resilience, adaptation and transformation assessment framework: from theory to application. GEN 2015.
Pagan, J., Pryor, M., Deepa, R., Grace III, J.M., Mbuya, O., Taylor, R., Dickson, Johnbull O., Ibeanusi, V., Chauhan, A., Chen, G., Anandhi, A., 2020. Sustainable Development Tool Using Meta-Analysis and DPSIR Framework — Application to Savannah River Basin, U.S. J. Am. Water Resour. Assoc. 1–24 (in press).
Pagliacci, F., Defrancesco, E., Mozzato, D., Bortolini, L., Pezzuolo, A., Pirotti, F., Pisani, E., Gatto, P., 2020. Drivers of farmers' adoption and continuation of climate-smart agricultural practices. A study from northeastern Italy. Sci. Total Environ. 710, 136345.
Pan, D., 1996. Soybean Responses to Elevated Temperature and Doubled CO2. Doctoral dissertation. University of Florida.
Pathak, T.B., Stoddard, C.S., 2018. Climate change effects on the processing tomato growing season in California using growing degree day model. Model. Earth Syst. Environ. 4, 765–775.
Peet, M.M., Sato, S., Gardner, R.G., 1998. Comparing heat stress effects on male-fertile and male-sterile tomatoes. Plant Cell Environ. 21, 225–231.
Peters, Glen P., Andrew, Robbie M., Boden, Tom, Canadell, Josep G., Ciais, Philippe, Corinne Le Quéré, Marland, Gregg, Raupach, Michael R., Wilson, Charlie, 2013. The challenge to keep global warming below 2 C. Nat. Clim. Change 3 (1), 4–6.
Pettigrew, W.T., 2008. The effect of higher temperatures on cotton lint yield production and fiber quality. Crop Sci. 48.
Prasad, P.V., Boote, K.J., Allen Jr, L.H., Thomas, J.M., 2002. Effects of elevated temperature and carbon dioxide on seed-set and yield of kidney bean (Phaseolus vulgaris L.). Global Change Biol. 8, 710–721.
Prasad, P.V.V., Boote, K.J., Allen Jr, L.H., 2006. Adverse high temperature effects on pollen viability, seed-set, seed yield and harvest index of grain-sorghum [Sorghum bicolor (L.) Moench] are more severe at elevated carbon dioxide due to higher tissue temperatures. Agric. For. Meteorol. 139, 237–251.
Ramos, R.S., Kumar, L., Shabani, F., Picanço, M.C., 2019. Risk of spread of tomato yellow leaf curl virus (TYLCV) in tomato crops under various climate change scenarios. Agric. Syst. 173, 524–535.
Reddy, K.R., Vara Prasad, P.V., Kakani, V.G., 2005. Crop responses to elevated carbon dioxide and interactions with temperature: cotton. J. Crop Improvement 13, 157–191.
Rockström, J., Karlberg, L., Wani, S.P., Barron, J., Hatibu, N., Oweis, T., Bruggeman, A., Farahani, J., Qiang, Z., 2010. Managing water in rainfed agriculture—the need for a paradigm shift. Agric. Water Manage. 97, 543–550.
Rotundo, J.L., Tang, T., Messina, C.D., 2019. Response of maize photosynthesis to high temperature: implications for modeling the impact of global warming. Plant Physiol. Biochem. 141, 202–205.
Ruane, A.C., McDermid, S., Rosenzweig, C., Baigorria, G.A., Jones, J.W., Romero, C.C., DeWayne Cecil, L., 2014. Carbon-Temperature-Water change analysis for peanut production under climate change: a prototype for the AgMIP Coordinated Climate-Crop Modeling Project (C3MP). Glob Change Biol. 20, 394–407.
Sanders, A., Thomas, T. S., Rios, A., & Dunston, S., 2019. Climate Change, Agriculture, and Adaptation Options for Honduras.
Sato, S., Peet, M.M., & Thomas, J.F., 2002. Determining critical pre-and post-anthesis periods and physiological processes in Lycopersicon esculentum Mill. exposed to moderately elevated temperatures. Journal of Experimental Botany 53, 1187-1195.
Schlenker, W., Roberts, M.J., 2009. Nonlinear temperature effects indicate severe damages to U.S. crop yields under climate change. PNAS 106 (37), 15594–15598.
Shah Chishti, S.A., Hussain, M.M., Imran, A., Nadeem, K., Saeed, A., Jalil, S., 2019. Temperature based crop modeling for round the year tomato production in Pakistan. J. Agric. Res. 03681157, 57.
Shahzad, M.F., Abdulai, A., 2020. Adaptation to extreme weather conditions and farm performance in rural Pakistan. Agric. Syst. 180.
Singh, R.P., Prasad, P.V., Sharma, A.K., Reddy, K.R., 2011. Impacts of High-Temperature Stress and Potential Opportunities for Breeding. Crop Adaptation to Climate Change, pp. 166–185.
Sinnathamby, S., Douglas-Mankin, K.R., Muche, M.E., Hutchinson, S.L., Anandhi, A., 2018. Ecohydrological index, native fish, and climate trends and relationships in the Kansas River basin. Ecohydrology 11, e1909.
Smit, B., Burton, I., Klein, R.J., Street, R., 1999. The science of adaptation: a framework for assessment. Mitig. Adapt. Strat. Glob. Change 4, 199–213.
Smit, B., Skinner, M.W., 2002. Adaptation options in agriculture to climate change: a typology. Mitig. Adapt. Strat. Glob. Change 7, 85–114.
Srivastava, A., Naresh Kumar, S., Aggarwal, P.K., 2010. Assessment on vulnerability of sorghum to climate change in India. Agric. Ecosyst. Environ. 138, 160–169.
Sterman, J., 2010. Business Dynamics. Irwin/McGraw-Hill c2000.
Thomas, J.M.G., 2001. Impact of Elevated Temperature and Carbon Dioxide on Development and Composition of Soybean Seed. Doctoral dissertation. University of Florida.
Usda-Nass, 2017. Crop production 2016 summary. United States Department of Agriculture – National Agricultural Statistics Service, Washington, DC, USA.
Vannevel, R., 2018. Using DPSIR and balances to support water governance. Water 10, 118.
Vara Prasad, P.V., Boote, K.J., Hartwell Allen, L., Thomas, J.M.G., 2003. Super-optimal temperatures are detrimental to peanut (Arachis hypogaea L.) reproductive processes and yield at both ambient and elevated carbon dioxide. Global Change Biol. 9, 1775–1787.
Ventrella, D., Charfeddine, M., Moriondo, M., Rinaldi, M., Bindi, M., 2012. Agronomic adaptation strategies under climate change for winter durum wheat and tomato in southern Italy: irrigation and nitrogen fertilization. Reg Environ Change 12, 407–419.
Voloudakis, D., Karamanos, A., Economou, G., Kalivas, D., Vahamidis, P., Kotoulas, V., Kapsomenakis, J., Zerefos, C., 2015. Prediction of climate change impacts on cotton yields in Greece under eight climatic models using the AquaCrop crop simulation model and discriminant function analysis. Agric. Water Manage. 147, 116–128.
Wahid, A., Gelani, S., Ashraf, M., Foolad, M., 2007. Heat tolerance in plants: an overview. Environ. Exp. Bot. 61, 199–223.
Wang, D., Heckathorn, S.A., Mainali, K., Tripathee, R., 2016. Timing effects of heat-stress on plant ecophysiological characteristics and growth. Front. Plant Sci. 7, 1629.
Yang, Y., Yang, Y., Han, S., Macadam, I., Liu, D.L., 2014. Prediction of cotton yield and water demand under climate change and future adaptation measures. Agric. Water Manage. 144, 42–53.
Zare, F., Elsawah, S., Bagheri, A., Nabavi, E., Jakeman, A.J., 2019. Improved integrated water resource modelling by combining DPSIR and system dynamics conceptual modelling techniques. J. Environ. Manage. 246, 27–41.
Zhang, C., Chen, X., Li, Y., Ding, W., Fu, G., 2018. Water-energy-food nexus: Concepts, questions and methodologies. J. Clean. Prod. 195, 625–639.